



Article

Design and Optimization of Coal to Hydrogen System Coupled with Non-Nominal Operation of Thermal Power Unit

Li Zhang ¹, Yu Zhang ¹ , Jianping Tang ¹, Lixia Kang ^{1,2,*} and Yongzhong Liu ^{1,2,*} ¹ Department of Chemical Engineering, Xi'an Jiaotong University, Xi'an 710049, China² Engineering Research Centre of New Energy System Engineering and Equipment, University of Shaanxi Province, Xi'an 710049, China

* Correspondence: lx_kang@mail.xjtu.edu.cn (L.K.); yzliu@mail.xjtu.edu.cn (Y.L.)

Abstract: In an actual thermal power plant, deep peak shaving will cause thermal power units to run under non-nominal conditions for an extended period, resulting in serious problems such as increased equipment wearing, low equipment utilization efficiency and decreased benefits. To this end, in this work, both the design and optimization method for a coal to hydrogen system which is coupled with the expected non-nominal operation of thermal power units are proposed. Aiming towards maximum profit in the context of thermal power plants, a mathematical optimization model for a coal to hydrogen system based on the multi-period operating conditions of thermal power plants is established. The corresponding optimal design scheme of the coal to hydrogen system is determined using variable operating conditions. The superiority of the integrated system compared with an independent system is explored and the feasibility of the proposed method is verified by using the case study of an actual thermal power plant. The results show that compared with the independent system, the economic benefits of the integrated system can increase by 13.56%, where the sale of hydrogen in the coal to hydrogen system accounts for 60.3% of the total benefit. The main expenditure associated with the system is the purchase cost of feedstock coal, accounting for 91.8%. Since the required power and medium-pressure steam in the coal to hydrogen process are provided by thermal power units, the minimum operating load of the thermal power plant in the integrated system increases from 40% to 60.1%, which significantly improves the utilization efficiency and service life of the generator units. In addition, the proposed integration scheme of the system is simple and controllable, which can contribute to the maintenance of the safe and stable operation of power generation and hydrogen production processes. These results are expected to provide the necessary methodological guidance for the integration and optimization of coal-fired power plants and coal to hydrogen systems.



Citation: Zhang, L.; Zhang, Y.; Tang, J.; Kang, L.; Liu, Y. Design and Optimization of Coal to Hydrogen System Coupled with Non-Nominal Operation of Thermal Power Unit. *Processes* **2022**, *10*, 2600. <https://doi.org/10.3390/pr10122600>

Academic Editor: Raymond Cecil Everson

Received: 22 September 2022

Accepted: 14 November 2022

Published: 5 December 2022

Publisher's Note: MDPI stays neutral with regard to jurisdictional claims in published maps and institutional affiliations.



Copyright: © 2022 by the authors. Licensee MDPI, Basel, Switzerland. This article is an open access article distributed under the terms and conditions of the Creative Commons Attribution (CC BY) license (<https://creativecommons.org/licenses/by/4.0/>).

Keywords: thermal power plant; coal to hydrogen system; multi-period integration; process simulation; system optimization

1. Introduction

In the context of carbon neutrality, the installed capacity and share of renewable energies, such as wind power, solar photovoltaic power and hydropower have risen rapidly. Existing thermal power units, especially large-scale coal-fired power plants, will face increasingly severe overcapacity and a decline in the annual available hours of power generation. In addition, the continuous rise in the price of coal will result in thermal power units participating in deep peak shaving [1]. However, the non-nominal operation of thermal power units in peak shaving processes will not only aggravate the wear and tear of devices and shorten their service life [2] but will also significantly increase coal and energy consumption [3] and reduce the economic benefits of thermal power plants. Therefore, seeking an economical and efficient operational mode that can adapt to the demand for

peak shaving will become the key to the green transformation and development of thermal power plants [4,5].

Integrating thermal power units with an energy storage system or chemical production system is expected to provide new ways of solving this problem [6–9]. In this method, thermal power units can integrate with the energy storage system or hydrogen production system through electricity, steam and devices, etc. [10]. In this way, the problems of device wear [11] and low utilization efficiency caused by the frequent start–stop of thermal power units are avoided, thus prolonging the service life of the unit and increasing the power load [12,13]. Furthermore, the method is also conducive to improving the capacity of thermal power units when participating in depth peak shaving [14]. In general, the surplus electricity of thermal power plants can be converted into other forms of energy for storage, which serves to balance fluctuations in electricity over different periods [15]. In addition, using the surplus electricity and heat of thermal power plants for combined chemical production is optimal for thermal power plants when participate in deep peak shaving [16–18].

Benalcazar [7] optimized the thermal energy storage unit in a combined heat and power plant. With the aim of addressing multiple heat sources, Zhang et al. [9] suggested a molten salt thermal storage system in a coal-fired power plant which helps to improve the flexibility of thermal power units and their ability to participate in peak shaving. Wang et al. [14] stored the heat of the surplus main steam and reheat steam of thermal power units via molten salt, and proved that energy storage systems can significantly enhance the deep peak shaving capacity of thermal power plants and overcome power load limitations. Thomas et al. [19] summarized the application and advantages of molten salt energy storage at commercial and research levels, and outlined the developmental potential of molten salt energy storage systems and their integration with power plants. Wolfersdorf et al. [20] pointed out that the minimum power load of a thermal power plant can be reduced from 50% to 33–34% by coupling thermal power units with their annex units for chemical energy storage. Pérez et al. [16] introduced combined heat and power generation and the biorefinery of biogas in a waste treatment plant, which significantly improved the flexibility of the power plant. Romeo et al. [21] integrated a thermal power plant with a power-to-gas (PtG) system via thermal coupling to avoid the frequent start–stop of thermal power units due to low loads, thereby reducing start–stop costs. It was shown that the integration of a thermal power plant and a PtG system can greatly reduce costs in terms of power production and frequent start–stops, therefore improving the economy of the thermal power plant. Forman et al. [8] integrated thermal power units with the syngas-based chemical synthesis system via thermal coupling, and it was suggested that the coal consumption of thermal power plants can be effectively reduced and the load elasticity of thermal power units can be greatly modified. In addition, a reduction in the start–stop frequency of thermal power plants and a minimum load in terms of the units was also achieved. Buttler et al. [15] introduced a hydrogen production system into an integrated gasification combined cycle power plant via water electrolysis. The results showed that the integrated system could not only significantly improve the operational flexibility and economic benefits of the power plant but also increase its capacity to participate in peak shaving.

Similar to the above-mentioned systems, such as the PtG system, the syngas system and the hydrogen production system via water electrolysis, the coal to hydrogen (CtH) system also has great potential to be integrated with thermal power units. On one hand, the CtH process adopts coal as the raw material to produce high-purity hydrogen, which requires a large amount of medium-pressure (MP) steam for gasification and water gas shift reactions [22,23]. Thus, under non-nominal operation conditions, the thermal power units can not only share the raw coal and cooling water system with the CtH system but also provide the MP reheat steam to CtH system [14]. On the other hand, the large amount of high-grade heat [24] generated in the CtH process can generate high-pressure (HP) steam to create additional benefits for the power plant. Therefore, the integration of thermal power

units with the CtH system can not only improve the operational flexibility of thermal power plants under the premise of meeting the peak shaving demand but also promote the economic benefits of power plants through hydrogen production and HP steam generation. The system provides an opportunity for energy conservation, emission reductions and the green transformation of coal-fired power plants and CtH systems. However, in most current research, thermal power units are commonly integrated with chemical production systems through electricity only, where the chemical production system is mainly used to consume the surplus electricity in a thermal power plant. In this way, the operations of the two systems are practically independent. In fact, coupling the two systems results in greater energy conservation, a reduction in emissions as well as economic and operational benefits. In addition, in such integrated systems, the chemical production system is usually designed on the basis of fixed operating conditions in terms of thermal power units, and little attention is paid to the design and operational characteristics of such integrated systems under variable operating conditions.

To address these problems, both an integrated system of thermal power units and a coal-to-hydrogen system coupled through electricity, steam and devices, etc., were constructed, and the effects of coupling the two systems in terms of energy conservation and material utilization as well as improvements in economic and operational benefits were explored. Additionally, with the consideration of the three typical non-nominal operating states of thermal power units, a multiperiod optimization model for the integrated system was established and solved to determine optimal design and operation schemes, so that the design and operation characteristics of the integrated system could be studied in the context of variable operating conditions. The superiority of the integrated system compared to the independent systems was studied and the results are expected to provide the necessary methodological guidance for the integration and optimization of coal-fired power plants and CtH systems.

2. Problem Statement

Figure 1 shows the integrated scheme of the thermal power plant and CtH system under non-nominal operational conditions, where the two systems are integrated via heat, steam and electricity. As shown in Figure 1, the feedstock coal enters the thermal power plant boiler and the CtH gasifier. HP steam produced in the boiler enters the thermal power units to generate electricity. MP steam is extracted from the thermal power units and is offered to the gasification and water gas shift sections of the CtH system, according to the demand for peak shaving. If the extracted MP steam is greater than the demand for the CtH process, the surplus can be sold directly. Meanwhile, the thermal power plant provides low-cost electricity to the CtH process under the condition of meeting the grid load demand. Since the required MP steam in the CtH system is satisfied by the thermal power units, the high-temperature waste heat generated in the CtH system can thus be used to produce HP steam, with this being sold together with the hydrogen. Finally, the boiler water consumed and the insufficient MP steam required in the CtH system can be externally purchased.

Note that in this work, the thermal power units are assumed to operate in a multiperiod condition according to the peak shaving demand of the power grid and the boiler is assumed to keep operating at full load in order to provide sufficient steam for the integrated system.

In this work, the primary design problem associated with the integrated system of a CtH system and thermal power units with variable operating conditions can be stated as follows: given there are (1) multiperiod operation parameters in terms of the thermal power plant, (2) cost parameters in terms of feedstock, hydrogen, steam and operational units and (3) a peak shaving demand, the aim is to determine the optimal design and operational scheme for the CtH system, including the optimal capacity allocation of the CtH system, the distribution of raw coal, steam, water and electricity and hydrogen production capacity in each period, in order to maximize the total profit of the integrated system.

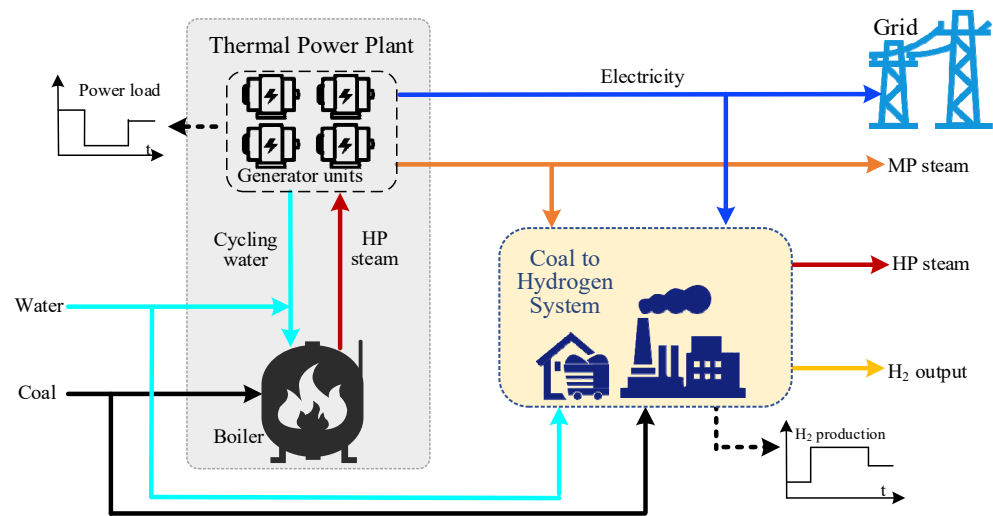


Figure 1. An integrated scheme of a thermal power plant and CtH system.

3. Mathematical Optimization Model of the Integrated System

3.1. Objective Function

The objective function is to maximize the annual profit (PRO) of the whole system, which is equal to the difference between the total revenue of the system and the total expenditure, as presented in Equation (1).

$$\max PRO = R_{ele} + R_{MPS} + R_{HPS} + R_{H_2} - C_{coal} - C_{water} - C_{cap} - C_{cop}, \quad (1)$$

where R_{ele} , R_{MPS} , R_{HPS} and R_{H_2} are the sale revenue in terms of electricity, MP steam, HP steam and hydrogen, respectively; C_{coal} and C_{water} are the costs of coal and water; and C_{cap} and C_{cop} are the annualized capital cost of the CtH system and the total operating cost of the integrated system.

The electricity revenue is related to the peak load of the power grid, which can be expressed as

$$R_{ele} = c^{ele} \sum_p W_{net,p}^{ele} T_p, \quad (2)$$

where c^{ele} is the price of electricity and $W_{net,p}^{ele}$ is the power input to the grid by the thermal power units in period p .

The sale revenue in terms of MP steam, HP steam and hydrogen can be calculated as

$$R_{MPS} = c^{MPS} \sum_p S_p^{MPS}, \quad (3)$$

$$R_{HPS} = c^{HPS} \sum_p S_p^{HPS}, \quad (4)$$

$$R_{H_2} = c^{H_2} \sum_p S_p^{H_2}, \quad (5)$$

where c^{MPS} , c^{HPS} and c^{H_2} are the prices of MP steam, HP steam and hydrogen, respectively and S_p^{MPS} , S_p^{HPS} and $S_p^{H_2}$ are the amount of sold MP steam, HP steam and hydrogen in period p .

The costs of feedstock coal and water, c^{coal} and c^{water} , can be calculated as

$$C_{coal} = c^{coal} \sum_p M_p^{coal}, \quad (6)$$

$$C_{water} = c^{water} \sum_p M_p^{water}, \quad (7)$$

where M_p^{coal} and M_p^{water} are the demands for coal and water in the p -th period, respectively.

The capital cost of the operation units in the CtH system can be calculated via the index factor method [25].

$$C_{cap} = Af \cdot \sum_u (1 + IC)(1 + BOP)C_{0,u} \left(\frac{\max(S_{u,p})}{S_{0,u}} \right)^{sf_u}, \quad (8)$$

where, Af is the annualized factor; BOP and IC are the cost factors related to device installation and indirect costs, which are assumed to be 0.32 and 0.2, respectively [25]; $C_{0,u}$ is the base cost of each operation unit and $S_{0,u}$ is the base case flow; $S_{u,p}$ is the cost flow; and sf is the scaling factor.

The operating cost, C_{cop} , of the system is associated with the total utilities, such as cooling and heating utilities, as well as the electricity consumed in the system.

$$C^{op} = \sum_{i=1}^p Q_{cu,p} c^{cu} + \sum_{i=1}^p Q_{hu,p} c^{hu} + \sum_{i=1}^p E_{ele,p} c^{ele}, \quad (9)$$

where $Q_{cu,p}$, $Q_{hu,p}$ and $E_{ele,p}$ are the amount of cooling utility, heating utility and electricity consumed in the p -th period and c^{cu} and c^{hu} are the prices in terms of cooling and heating utilities.

3.2. Constraints

(1) Mass balance of MP steam

The MP steam extracted from the thermal power units can be input to the CtH system or be sold directly, which is expressed as

$$M_{tur,p}^{MPS} = M_{CtH,p}^{MPS} + S_p^{MPS}, \quad (10)$$

where $M_{tur,p}^{MPS}$ is the amount of MP steam extracted from the thermal power units; $M_{CtH,p}^{MPS}$ is the amount of MP steam input to the CtH system and S_p^{MPS} is the amount of MP steam sold.

The amount of steam extracted from the thermal power units should be less than that generated in the boiler, $M_{tot,p}^S$, which can be formulated as

$$M_{tur,p}^{MPS} \leq M_{tot,p}^S, \quad (11)$$

(2) Mass balance of boiler water

Water is purchased externally and used to compensate for the reduction in water due to steam extraction and sales, which can be expressed as

$$M_p^{water} = S_p^{HPS} + M_{tur,p}^{MPS}, \quad (12)$$

(3) Mass balance of raw coal

The total amount of coal entering the system, M_p^{coal} , is equal to the sum of the amount of coal entering the boiler, $M_{boil,p}^{coal}$ and the gasifier, $M_{CtH,p}^{coal}$.

$$M_p^{coal} = M_{boil,p}^{coal} + M_{CtH,p}^{coal}, \quad (13)$$

(4) Power balance

In each period, the power generated by thermal power units, $W_{tub,p}^{ele}$, can be allocated to the CtH system, $W_{H_2,p}^{ele}$, and the grid, $W_{net,p}^{ele}$.

$$W_{turb,p}^{ele} = W_{net,p}^{ele} + W_{H_2,p}^{ele}, \quad (14)$$

where the power input to the grid is determined by the peak shaving requirement,

$$W_{net,p}^{ele} = \eta_p W^{\max}, \quad (15)$$

where η_p is grid peaking power factor and W^{\max} is the full load power of thermal power plant. The electricity consumed in CtH system is expressed as

$$W_{H_2,p}^{ele} = W_{AUS,p}^{ele} + W_{COMP,p}^{ele} + W_{Refg,p}^{ele} \quad (16)$$

where $W_{AUS,p}^{ele}$, $W_{COMP,p}^{ele}$ and $W_{Refg,p}^{ele}$ are the electricity consumed by the air separation unit, compressors and low temperature refrigeration unit, respectively.

Since the boiler is assumed to be in full-load operation, the amount of steam generated is constant and determined by the given amount of coal. For thermal power units, the extraction of MP steam does not affect the power generation of the high-pressure turbine. Therefore, the output power of the turbine can be related to the coal consumption of the boiler, as presented in Equation (17)

$$W_{turb,p}^{ele} = W_{HPturb}^{ele} + \lambda^{tur} (M_{tot,p}^s - M_{turb,p}^{MPS}), \quad (17)$$

where λ^{tur} is the relationship coefficient that can be obtained through multiple simulations. A detailed simulation can be found in Appendix A.

(5) Constraints terms of cost and material flows in the CtH system

To simplify the calculations, the relationships between the parameters and the amount of feedstock coal in the CtH system should be first determined. To this end, a detailed simulation of the CtH system is first performed under steady-state conditions, where the reaction process reaches equilibrium and the degree of separation remains constant, as can be found in Appendix A. The quantitative relationship between the cost flows, the hydrogen production, the electricity consumption, the amount of HP steam and MP steam and the amount of feedstock coal, $M_{CtH,p}^{MPS}$, is then determined through polynomial regression according to the sensitivity analysis of the simulation process, as shown in Equation (18).

$$\begin{cases} f = k M_{CtH,p}^{coal} \\ f = S_{u,p}, S_p^{H_2}, W_{H_2,p}^{ele}, S_p^{HPS}, M_{CtH,p}^{MPS} \end{cases} \quad (18)$$

where k stands for the regression coefficient.

Thus, the solution procedure of this work can be summarized as follows: An integrated scheme of thermal power units and a coal-to-hydrogen system was first constructed. Then, the integrated system was simulated under three typical non-nominal operation states in terms of thermal power units to quantitatively relate the cost flows, hydrogen production, electricity consumption and amount of steam to the amount of feedstock coal in the CtH system, as presented in Equation (18). In what follows, a multi-period optimization model was established by taking the maximum annual profit (PRO) of the whole system as the objective function and the energy balances, mass balances and operational constraints of the integrated system as the constraints. Finally, by solving this model, an optimal design for a coal-to-hydrogen system that enables it to adapt to the three non-nominal operation states (corresponding to three operating periods) was determined. The output of the model includes the required amounts of coal and MP steam, the production of hydrogen and HP steam in each period as well as the total annual profit of the whole system.

4. Case Study

4.1. Fundamental Data

In this section, the thermal power units from an actual 330 MW thermal power plant in China were applied to verify the effectiveness of the proposed method. Table 1 shows the fundamental data of coal in the power plant. It was known that under the nominal

load, the coal input to the boiler was 122 t/h and the amount of HP steam generated was 916.6 t/h. Thermal power plant was assumed to operate in the three periods during its participation in peak shaving, where the electricity input to the grid was 75% of the full load from January to March, 40% from April to September and 60% from October to December.

Table 1. Industrial and elemental analysis of coal.

Industrial Analysis/%					Elemental Analysis/%				LHV MJ/kg
Mt	Aar	VM	FC	C	H	N	S	O	
8.5	18.3	30.7	51	58	4.0	1.0	1.0	11.5	23.007

Other computational parameters included: the cost of the electricity input to grid, which was 0.1492 \$/kWh; the cost of coal and hydrogen were 223 \$/t and 2.238 \$/kg; the costs of MP steam and HP steam were 32.8 \$/t and 38.7 \$/t; and the price of water was 0.6109 \$/t. All these parameters were determined according to their market price in China. The capital cost parameters of each operational unit in the CtH system are summarized in Table 2. The regression coefficients of the relevant parameters in the CtH system are listed in Table 3.

Table 2. Cost parameters in the CtH system [25].

Unit	$C_{o,u}$ (MM\$)	$S_{ref,u}$	sf_u	Cost Flow Basis
Coal mill	50.43	161.7	0.65	Coal feed (kg/s)
Coal gasifier	51.2	17.94	0.7	Coal feed (kg/s)
Compressor	6.93	10	0.67	Power (MW)
Forward shift reactor	3.47	150	0.67	Feed (kg/s)
Rectisol CO ₂ removal unit	29.77	2.51	0.63	Feed gas (kmol/s)
PSA	7.38	0.29	0.65	Purge gas (kmol/s)
Refrigerator	1.19	0.7	0.7	Heat removed (MW)
ASU	130.77	145	0.5	O ₂ feed (kg/s)

Table 3. Regression coefficients of the parameters in the CtH system.

Parameters		k
$S_{u,p}$	Coal mill	0.2778
	Coal gasifier	0.2778
	Compressor	0.0711
	Forward shift reactor	0.9952
	Rectisol CO ₂ removal unit	0.0333
	PSA	0.0197
	Refrigerator	0.0594
$S_p^{H_2}$	ASU	0.1521
	H ₂ production	0.1433
$W_{H_2,p}^{ele}$	Power requirement	0.2745
S_p^{HPS}	HP steam output	2.0512
$M_{CtH,p}^{MPS}$	MP steam requirement	1.8601

Note that the optimization model determined by Equations (1)–(18) is a nonlinear programming (NLP) model. The General Algebraic Modeling System (GAMS) platform was used to solve the model with BARON as the solver.

4.2. Design Characteristics of the Integrated System

By solving the multi-period optimization model proposed in this work, an optimal design scheme of the CtH system was obtained. According to the results, the hydrogen

production is 268,494 t/y and the total coal consumption is 2,943,141 t/y, with the maximum profit being 226.54 MM\$. Figure 2 provides cost breakdown of the whole system.

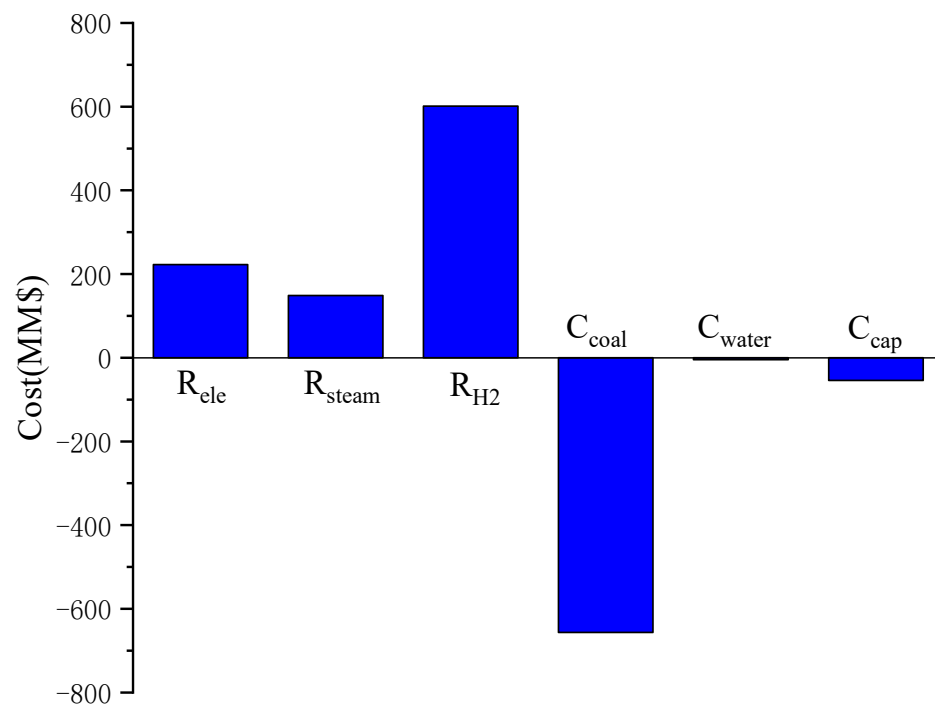


Figure 2. Breakdown of the costs of the integrated system.

It can be seen from Figure 2 that the main revenue of the integrated system comes from the sale of hydrogen, which is 601.17 MM\$, accounting for 60.3% of the total revenue. The sale of electricity to the grid is in the second place, at 222.54 MM\$. At the same time, the sale of HP steam produced by waste heat during the CtH process results in a benefit of 148.8 MM\$. The results in Figure 2 also show that the purchase cost of raw coal is 656.35 MM\$, accounting for more than 90% of the total cost. The coal price used is at a high level, 223 \$/t, due to environmental protections and economic requirements. The annual capital cost of the CtH system is 54.12 MM\$, and the make-up water is the lowest factor in terms of costs. It is worth noting that the operating cost of the integrated system, including heating and cooling utilities and electricity, is zero. This is because, the integrated system does not require heating utilities. Besides, the electricity required in the CtH process is entirely provided by thermal power units, and the required cooling water is provided by the cooling system of the thermal power units.

4.3. Operation Characteristics of the Integrated System

Table 4 provides a multi-period operational scheme of the integrated system. According to the peak shaving demand, the thermal power units operate in the three periods with loads of 75%, 40% and 60% and with durations of 2190 h, 4380 h and 2190 h, respectively. Considering that the boiler in the thermal power plant keeps operating in full-load state, the total coal consumption is fixed at 1,068,720 t/y. The on-grid load of the power plant is 1,492,704 MWh determined by the given demand of peak shaving.

Table 4. Multi-period operating parameters of the integrated system.

Period		P1	P2	P3	Total/t
Coal to boil	Total (t)	267,180	534,360	267,180	1,068,720
	Rate (t/h)	122	122	122	
Coal to CtH system	Total (t)	270,903	1,193,112	410,406	1,874,421
	Rate (t/h)	123.7	272.4	187.4	
Electricity to net	Total (MWh)	520,782	555,384	416,538	1,492,704
	Rate (MW)	237.8	126.8	190.2	
Electricity to CtH system	Total (MWh)	742,41	327,624	112,566	514,431
	Rate (MW)	33.9	74.8	51.4	
MP steam to CtH system	Total (t)	503,919	2,216,718	763,434	3,484,071
	Rate (t/h)	230.1	506.7	348.6	
MP steam output	Total (t)	0	0	0	0
	Rate (t/h)	0	0	0	
HP steam output	Total (t)	555,603	2,447,544	841,836	3,844,983
	Rate (t/h)	253.7	558.8	384.4	
H2 production	Total (t)	38,763	170,820	58,911	268,494

It can be seen in Table 4 that the total coal consumption of the CtH process is 1,874,421 t/y, where period 2 consumes the most, followed by period 3, with period 1 consuming the least. The total amount of steam generated by the thermal power plant is 916.6 t/h, and the on-grid load of the thermal power units is 40% in period 2, 60% in period 3 and 75% in period 1. It can be seen that the trend in terms of coal consumption in the CtH system is exactly opposite to that of the on-grid load of the thermal power units. This means the smaller the on-grid load of the thermal power units is, the more coal will be fed to the CtH system. The smaller the on-grid load of thermal power units is, the less steam will be consumed and the greater the amount of MP steam provided to the CtH system will be.

As shown in Table 4, when the on-grid load reaches the lowest—40% of the nominal load in period 2, the amount of MP steam extracted from the thermal power units is as high as 506.7 t/h. In this case, the capacities of the gasification and water gas shift processes in CtH system increase significantly and the coal consumption of the system reaches its maximum. As a result, the hydrogen production and power consumption of the CtH system, as well as the HP steam generated by it, reach their maximum. In this period, the amount of hydrogen production is 39 t/h, the by-product HP steam is 558.8 t/h and the power consumption is 74.8 MW. The total amount of hydrogen produced is 268,494 t/y and the HP steam is 3,844,983 t/y, with a total power consumption of 514,431 MWh.

The results in Table 4 also show that, in all periods, the MP steam extracted from the thermal power units is allocated to the CtH system without being sold and the maximal flow rate of 506.7 t/h is reached in period 2. Since the amount of MP steam extracted from the thermal power units is closely related to the on-grid load and the power consumption of the CtH system, the distribution of steam is also considered the best trade-off between the revenue and capital costs of the system.

4.4. Further Discussion

To verify the superiority of the integrated system proposed in this work in terms of its economy and operation, in this section, a comprehensive comparison of the integrated system and the independent systems was conducted. The results are summarized in Tables 5 and 6. Note that to unify the basis of comparison, the on-grid electricity load and the hydrogen production were the same in both the integrated system and the independent systems in the following two scenarios.

Table 5. Comparison of the integrated system and independent systems under fixed conditions.

Condition	75%THA			60%THA			40%THA		
System	Thermal power plant	CtH	Integrated system	Thermal power plant	CtH	Integrated system	Thermal power plant	CtH	Integrated system
Boiler load	75%	/	100%	60%	/	100%	40%	/	100%
Power generator load	75%	/	82.3%	60%	/	73.2%	40%	/	61.1%
Coal consumption (t)	801,540	1,083,612	2,152,332	641,232	1,641,624	2,710,344	427,488	2,386,224	3,454,944
Water consumption (t)	687	0	4,238,725	549.6	0	6,421,497	366.4	0	9,334,112
MP steam consumption (t)	0	2,015,626	2,015,626	0	3,053,585	3,053,585	0	4,438,615	4,438,615
H ₂ production (t)	/	155,052	155,052	/	235,644	235,644	/	341,640	341,640
HP steam output (t)	/	0	2,222,412	/	0	3,367,344	/	0	4,895,088
Profit (MM\$)	131.36	18.04	176.32	105.04	69.40	213.28	70.02	144.42	258.60

Table 6. Comparison between the proposed integration system and independent systems.

System	Proposed Integrated System	Thermal Power Plant	CtH System
Boil load	100%/100%/100%	75%/40%/60%	0
Power generator load	82.3%/61.1%/73.2%	75%/40%/60%	0
Coal consumption (t)	2,943,141	574,437	1,874,421
H ₂ production (t)	268,494	0	268,494
HP steam output (t)	3,844,983	0	0
Profit (MM\$)	226.54	105.4	94.08
Hydrogen production cost (\$/tH ₂)	11,204.11	-	12,620.51

4.4.1. Scenario 1: The Operating Condition of the Thermal Power Units Is Fixed

It can be seen that for the given operating condition of the thermal power plant, both the boiler and thermal power units operate in a non-nominal state, which greatly reduces the life and the utilization efficiency of the devices. In contrast, the integrated system can maintain the full-load operation of the boiler and increase the utilization efficiency of thermal power units, thereby reducing the wear and tear of the devices. According to Table 5, under a 40% turbine heat acceptance (THA) operation condition, the utilization efficiency of thermal power units increases from 40% to 61.1%, which effectively prevents the thermal power units operating at the minimum load for an extended period.

In addition, the integrated system is superior compared to the independent CtH system. Firstly, an independent CtH system can achieve a certain degree of self-sufficiency in terms of MP steam on the basis of internal heat integration, but the surplus waste heat can only be used to generate electricity to satisfy a portion of the power demand. In other words, even though the process waste heat can be fully used within the system, the system still requires high-priced MP steam and industrial electricity to be purchased externally [26]. By contrast, in the integrated system, both the MP steam and the electricity required in the CtH system can be provided by the thermal power plant, and the waste heat in the CtH system can further generate HP steam for sale. In this way, the capital costs of the MP steam and electricity are reduced, and additional revenue is created by selling high-level HP steam. Note that in the integrated system, the coal consumption is larger than the sum of that in the two separated systems. This is because, for the given peaking shaving demand, the thermal power plant in the integrated system will not only provide on-grid power but also supply low-cost electricity and MP steam to the CtH system. In this way, the total output power and amount of MP steam of the thermal power plant increases, leading to an

increase in the coal consumption. However, in separated systems, electricity and MP steam are purchased externally, which is costly. For all that, only the surplus steam and electricity in the thermal power plant are allocated to the CtH system for hydrogen production. The results in Table 5 show that the profit of the integrated system is about 20% higher than the sum of the profits of the independent thermal power plant and CtH systems.

4.4.2. Scenario 2: The Operating Condition of the Thermal Power Plant Is Variable

Table 6 provides a comparison of the results obtained by the independent systems and the integrated system under variable operating conditions. It can be seen that, in spite of the advantages in improving the utilization efficiency of the thermal power units, the integrated system reduces the cost of hydrogen production by 11.22% and increases the profits by 13.56%, when compared with the independent systems. In addition, it should be noted that in the design scheme of the integrated system, the two systems are mainly coupled via the power network and the steam pipelines, which are simple, flexible and controllable. Especially when compared with the heat integration of process streams, the proposed integrated scheme will have only a minor influence on the power generation process of thermal power units and the production process of the CtH system.

5. Conclusions

To counter the problems of low utilization efficiency and a reduction in benefits in the context of thermal power plants caused by their participation in power grid peak shaving, an optimal design method for an integrated system of a CtH and thermal power units under non-nominal conditions is proposed. Aiming to improve the benefits of the system and the utilization efficiency of thermal power units, the mathematical optimization model was developed and the application of the proposed method was verified via a case study of a practical industrial plant. The following conclusions can be drawn.

(1) The operation of the CtH system is closely related to the on-grid load of thermal power units, and the capacity of the CtH system is inversely proportional to the on-grid load of thermal power units.

(2) The total profit of the integrated system is 226.54 MM\$, where 60.3% comes from the sale of hydrogen, and the main cost of the system is attributed to the purchase cost of raw coal, which accounts for 91.8% of the total cost.

(3) Compared with independent systems, the integrated system can maintain the full-load operation of the boiler and increase the utilization efficiency of thermal power units, thereby reducing the wear and tear of devices.

(4) In addition to increasing the fixed on-grid power revenue, the integrated system can also produce hydrogen and generate additional HP steam. The profit of the integrated system is approximately 20% higher than the sum of the profits of independent systems under fixed operating conditions and is approximately 13.56% higher under the variable non-nominal operating conditions.

(5) Since the thermal power units and CtH systems are integrated via the power network and steam pipelines rather than employing internal heat integration, the proposed integrated scheme will have only a minor influence on the power generation process of the thermal power units and the production process of the CtH system.

In the context of carbon neutrality, our future work will primarily focus on the quantitative analysis of the CO₂ flows of the integrated system and the techno-economic evaluation of the coupling of the integrated system in terms of CO₂ capture, utilization and storage (CCUS) units.

Author Contributions: Conceptualization, L.K. and Y.L.; methodology, L.K., L.Z. and J.T.; software, L.Z. and Y.Z.; validation, L.Z. and L.K.; formal analysis, L.Z., Y.Z. and L.K.; investigation, L.Z., Y.Z. and L.K.; resources, L.K. and Y.L.; data curation, L.Z. and Y.Z.; writing—original draft preparation, L.Z., J.T. and Y.Z.; writing—review and editing, L.K.; visualization, L.Z. and L.K.; supervision, L.K. and Y.L.; project administration, L.K. and Y.L.; funding acquisition, L.K. and Y.L. All authors have read and agreed to the published version of the manuscript.

Funding: The authors gratefully acknowledge funding from the Key Research and Development Project of Shaanxi Province (No. 2022GY-185 and No. 2022GY-197) and projects (No. 21878240) sponsored by the National Natural Science Foundation of China (NSFC).

Data Availability Statement: Not applicable.

Conflicts of Interest: The authors declare no conflict of interest.

Appendix A Simulation of CtH

Figure A1 provides the simulation scheme of the CtH, where a coal gasification unit, a water gas shift unit, a rectisol CO₂ removal unit and a pressure swing adsorption (PSA) unit are included. Considering that coal is an unconventional component, its thermal decomposition section is modeled with the RYield block in Aspen plus. The model selection of the rest units is summarized in Table A1, and the simulation results are given in Table A2. Since this process involves weak polar and non-polar mixtures, the PR-BM property method [27] is adopted in coal gasification and water gas shift sections, and PSRK is used in the Rectisol CO₂ removal section [28]. The assumptions used in the simulations include:

- (1) all the reactions involved in the system have reached reaction equilibrium and phase equilibrium;
- (2) the gas and solid phases are separated completely, and the separation process occurs instantaneously;
- (3) the pressure drops of all the operation units are ignored.

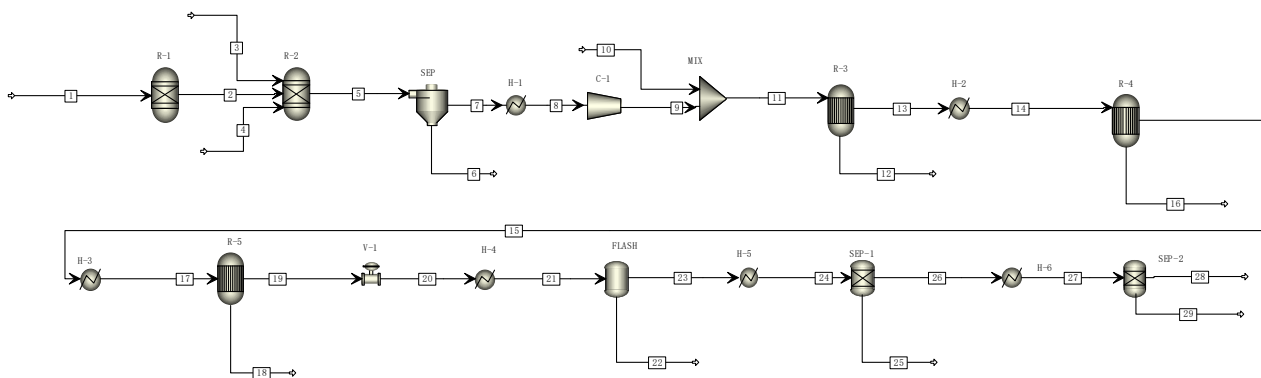


Figure A1. CtH process.

Table A1. Models and parameters adopted in the CtH simulation process.

Process	Name	Aspen Model	Operating Condition
Gasification	R-1	RYield	Operating pressure: 3 MPa; operating temperature: 700 °C
	R-2	RGibbs	Operating pressure: 3 MPa; operating temperature: 1400 °C
	SEP	Ssplit	Splitting rate: 1
	H-1	Heater	Cool to the target temperature
	C-1	Compr	Discharge pressure: 6.2 MPa; η isentropic: 0.85
Water gas shift	MIX	Mixer	-
	R-3	REquil	Operating pressure: 6.2 MPa; heat loss: 0 MW
	H-2	Heater	Cool to the target temperature
	R-4	REquil	Operating pressure: 6.05 MPa; heat loss: 0 MW
	H-3	Heater	Cool to the target temperature
Rectisol CO ₂ removal unit	R-5	REquil	Operating pressure: 5.94 MPa; heat loss: 0 MW
	V-1	Valve	Discharge pressure: 3.45 MPa
	H-4	Heater	Cool to the target temperature
	FLASH	Flash	Operating pressure: 3.45 MPa; operating temperature: 30 °C
	H-5	Heater	Cool to the target temperature
PSA	SEP-1	Sep	CO ₂ split fraction: 0.97
	H-6	Heater	Heat to the target temperature
	SEP-2	Sep	H ₂ split fraction: 0.995

Table A2. Simulate Stream Results.

Stream	T/°C	P/MPa	Mass Flow/kg·h ⁻¹	Stream	T/°C	P/MPa	Mass Flow/kg·h ⁻¹
1	25	0.1	68,000	16	0	0	0
2	700	3	68,000	17	240.4	5.94	219,876
3	300	4.75	1531.29	18	0	0	0
4	150	3.85	37,228.7	19	245.2	5.94	219,876
5	1400	3	106,760	20	237.8	3.45	219,876
6	1400	3	11,007.9	21	30	3.45	219,876
7	1400	3	95,752.1	22	30	3.45	67,114.3
8	164	3	95,752.1	23	30	3.45	152,761
9	280	6.2	95,752.1	24	−21	3.3	152,761
10	280	6.2	124,124	25	−21	3.3	142,353
11	263.1	6.2	219,876	26	−21	3.3	10,408.8
12	0	0	0	27	25	3.3	10,408.8
13	487	6.2	219,876	28	25	3.3	10,397
14	264.9	6.05	219,876	29	25	3.3	29.83
15	299.4	6.05	219,876				

The simulation results were compared with those in the literature, as shown in Tables A3 and A4. Table A3 shows the gas composition at the outlet of a coal gasification unit, and Table A4 presents the temperatures, pressures and the CO conversion rate of the three-stage adiabatic conversion process in a water gas shift unit. It can be seen that the relative errors between the simulation results and those reported in the literature are less than 5%, indicating the effectiveness and reliability of the simulations. Note that the content of CO₂ in Table A3 is relatively large because of the higher carbon content in feedstock coal.

Table A3. Validation of simulation results of gasification.

	Mole Fraction %				
	CO	H ₂	CO ₂	CH ₄	H ₂ S
Song et al. [29]	62.72	30.27	1.39	0.04	1.12
This work	60.41	31.59	1.48	0.04	1.17
Error %	3.68	4.36	6.47	0	4.46

Table A4. Validation of water gas shift.

Item		Reactor 1		Reactor 2		Reactor 3		Conversion Rate of CO %
T/°C	Wang et al. [26]	280.0	447.5	264.9	298.1	240.4	246.2	
	This work	278.8	487.5	264.9	294.2	240.4	243.8	
P/MPa	Wang et al. [26]	6.20		6.05		5.94		97.89
	This work	6.20		6.05		5.94		98.78

Figure A2 shows the simulation scheme of 330 MW thermal power units, and the models and parameters adopted in the simulation are summarized in Table A5. Since only water/steam is used in this process, the STEAMNBS property method was selected for the simulation. Table A6 shows a comparison of the simulation results with those in an actual plant. It can be seen that the relative error between the simulation results and original results are for the most part less than 5%, indicating the reliability and effectiveness of the simulations.

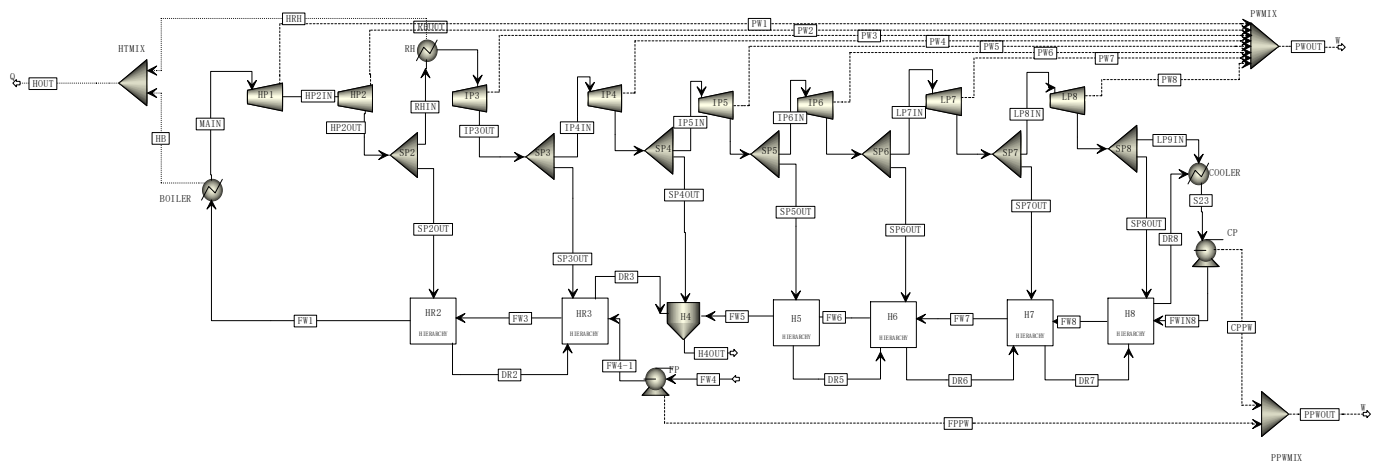


Figure A2. Thermal power units process.

Table A5. Models and parameters adopted in the thermal power unit simulation process.

Name	Aspen Model	Operating Condition
BOILER	Heater	Operating pressure: 17.77 MPa; operating temperature: 546.6 °C
RH	Heater	Operating pressure: 3.89 MPa; operating temperature: 548.6 °C
HP1~2/IP3~6/LP 7~8	Compr/Turbine	η isentropic: 0.91
SP 2~8	Fsplit	Turbine extraction
HT/PW/PPWMIX	Mixer	Power and heat generated during operation
COOLER	Heater	Operating temperature: 33 °C, gas fraction: 0
CP	Pump	Operating pressure: 1.74 MPa, η isentropic: 0.83
FP	Pump	Operating pressure: 17.7 MPa, η isentropic: 0.83
HR2~3/H5~8	Hierarchy/Heater	Heat to the target temperature

Table A6. Verification of simulation results of thermal power units.

Item	Temperature/°C		Error /%	Item	Temperature/°C		Error /%	Item	Temperature/°C		Error /%
	Simulation	Original			Simulation	Original			Simulation	Original	
FW1	254.56	254.77	0.08	SP1OUT	324.71	328.46	1.14	DR2	204.75	215.39	4.94
FW3	208.32	210.17	0.88	SP3OUT	449.61	463.51	2.99	DR3	183.52	192.38	4.61
FW4	179.01	178.94	0.04	SP4OUT	338.65	336.52	0.63	DR4	175.23	179.09	2.16
FW5	149.21	148.62	0.40	SP5OUT	233.03	269.64	13.58	DR5	117.58	117.97	0.33
FW6	100.52	101.23	0.70	SP6OUT	127.16	136.29	6.70	DR6	88.36	90.23	2.07
FW7	82.61	84.29	1.99	SP7OUT	87.37	85.72	1.92	DR7	78.30	74.85	4.61
FW8	59.89	64.62	7.32	SP8OUT	63.22	64.59	2.12	-	-	-	-

References

- Dong, Y.; Jiang, X.; Liang, Z.; Yuan, J. Coal power flexibility, energy efficiency and pollutant emissions implications in China: A plant-level analysis based on case units. *Resour. Conserv. Recy.* **2018**, *134*, 184–195. [\[CrossRef\]](#)
- Mertens, N.; Alobaid, F.; Starkloff, R.; Epple, B.; Kim, H.-G. Comparative investigation of drum-type and once-through heat recovery steam generator during start-up. *Appl. Energy* **2015**, *144*, 250–260. [\[CrossRef\]](#)
- Huang, C.; Zhang, P.; Wang, W.; Huang, Z.; Lyu, J.; Liu, J.; Yue, G.; Ni, W. The upgradation of coal-fired power generation industry supports China's energy conservation, emission reduction and carbon neutrality. *Ther. Power Gener.* **2021**, *50*, 1–6.
- Luo, X.; Wang, J.H.; Dooner, M.; Clarke, J. Overview of current development in electrical energy storage technologies and the application potential in power system operation. *Appl. Energy* **2015**, *137*, 511–536. [\[CrossRef\]](#)
- Yin, S.Y.; Zhang, S.F.; Andrews-Speed, P.; Li, W. Economic and environmental effects of peak regulation using coal-fired power for the priority dispatch of wind power in China. *J. Clean. Prod.* **2017**, *162*, 361–370. [\[CrossRef\]](#)

6. Xu, Y.Q.; Lu, B.W.; Luo, C.; Wu, F.; Li, X.S.; Zhang, L.Q. Na₂CO₃ promoted CaO-based heat carrier for thermochemical energy storage in concentrated solar power plants. *Chem. Eng. J.* **2022**, *435*, 134852. [\[CrossRef\]](#)
7. Benalcazar, P. Sizing and optimizing the operation of thermal energy storage units in combined heat and power plants: An integrated modeling approach. *Energy Convers. Manag.* **2021**, *242*, 114255. [\[CrossRef\]](#)
8. Forman, C.; Gootz, M.; Wolfersdorf, C.; Meyer, B. Coupling power generation with syngas-based chemical synthesis. *Appl. Energy* **2017**, *198*, 180–191. [\[CrossRef\]](#)
9. Zhang, K.Z.; Liu, M.; Zhao, Y.L.; Yan, H.; Yan, J.J. Design and performance evaluation of a new thermal energy storage system integrated within a coal-fired power plant. *J. Energy Storage* **2022**, *50*, 104335. [\[CrossRef\]](#)
10. Li, S.; Jin, H.G.; Gao, L. Cogeneration of substitute natural gas and power from coal by moderate recycle of the chemical unconverted gas. *Energy* **2013**, *55*, 658–667. [\[CrossRef\]](#)
11. Benato, A.; Bracco, S.; Stoppato, A.; Mirandola, A. LTE: A procedure to predict power plants dynamic behaviour and components lifetime reduction during transient operation. *Appl. Energy* **2016**, *162*, 880–891. [\[CrossRef\]](#)
12. Xu, J.; Bi, D.P.; Ma, S.X.; Bai, J. A data-based approach for benchmark interval determination with varying operating conditions in the coal-fired power unit. *Energy* **2020**, *211*, 118555. [\[CrossRef\]](#)
13. Wang, Z.J.; Gu, Y.J.; Liu, H.C.; Li, C.Y. Optimizing thermal-electric load distribution of large-scale combined heat and power plants based on characteristic day. *Energy Convers. Manag.* **2021**, *248*, 114792. [\[CrossRef\]](#)
14. Hui, W.; Jian, W. Research on the Energy Storage Technique by Steam Extraction from Thermal Power Units used to Deep Load Modulation. *Electr. Power Surv. Des.* **2022**, *6*, 30–34.
15. Buttler, A.; Kunze, C.; Spliethoff, H. IGCC-EPI: Decentralized concept of a highly load-flexible IGCC power plant for excess power integration. *Appl. Energy* **2013**, *104*, 869–879. [\[CrossRef\]](#)
16. Pérez, V.; Lebrero, R.; Muñoz, R. Comparative Evaluation of Biogas Valorization into Electricity/Heat and Poly(hydroxyalkanoates) in Waste Treatment Plants: Assessing the Influence of Local Commodity Prices and Current Biotechnological Limitations. *ACS Sustain. Chem. Eng.* **2020**, *8*, 7701–7709. [\[CrossRef\]](#)
17. Zhou, Z. Design of a System Coupling Liquid Air Energy Storage System with Thermal Power Unit. In Proceedings of the International Conference on Materials Chemistry and Environmental Engineering (CONF-MCEE 2021), Palo Alto, CA, USA, 7 November 2021.
18. Beiron, J.; Montanes, R.M.; Normann, F.; Johnsson, F. Combined heat and power operational modes for increased product flexibility in a waste incineration plant. *Energy* **2020**, *202*, 117696. [\[CrossRef\]](#)
19. Bauer, T.; Odenthal, C.; Bonk, A. Molten Salt Storage for Power Generation. *Chem. Ing. Tech.* **2021**, *93*, 534–546. [\[CrossRef\]](#)
20. Wolfersdorf, C.; Boblenz, K.; Pardemann, R.; Meyer, B. Syngas-based annex concepts for chemical energy storage and improving flexibility of pulverized coal combustion power plants. *Appl. Energy* **2015**, *156*, 618–627. [\[CrossRef\]](#)
21. Romeo, L.M.; Peña, B.; Bailera, M.; Lisbona, P. Reducing cycling costs in coal fired power plants through power to hydrogen. *Int. J. Hydrogen Energy* **2020**, *45*, 25838–25850. [\[CrossRef\]](#)
22. Chen, W.-H.; Chen, C.-Y. Water gas shift reaction for hydrogen production and carbon dioxide capture: A review. *Appl. Energy* **2020**, *258*, 114078. [\[CrossRef\]](#)
23. Crnomarkovic, N.; Repic, B.; Mladenovic, R.; Neskovic, O.; Veljkovic, M. Experimental investigation of role of steam in entrained flow coal gasification. *Fuel* **2007**, *86*, 194–202. [\[CrossRef\]](#)
24. Dorofeenko, S.O.; Polianczyk, E.V. Gasification of pulverized coal in a counterflow moving bed filtration combustion reactor: In search of the optimum. *Fuel* **2021**, *291*, 120255. [\[CrossRef\]](#)
25. Demirhan, C.D.; Tso, W.W.; Powell, J.B.; Pistikopoulos, E.N. Sustainable ammonia production through process synthesis and global optimization. *AIChE. J.* **2019**, *65*, 16498. [\[CrossRef\]](#)
26. Zhaocheng, W.; Yuyan, Q.; Baolin, Z.; Fanrong, L. Comparison and analysis of water gas shift processes matching for hydrogen production based on coal water slurry gasification. *Mod. Chem. Ind.* **2018**, *38*, 231–236.
27. Wan, W.; Dai, Z.; Li, C.; Yu, G.; Wang, F. Innovative concept for gasification for hydrogen based on the heat integration between water gas shift unit and coalewatereslurry gasification unit. *Int. J. Hydrogen Energy* **2014**, *39*, 7811–7818. [\[CrossRef\]](#)
28. Sun, L.; Smith, R. Rectisol wash process simulation and analysis. *J. Clean Prod.* **2013**, *39*, 321–328. [\[CrossRef\]](#)
29. Song, Z.C.; Bao, W.R.; Chang, L.P.; Fan, L.I. Entrained-flow pulverized coal gasification performance simulation analysis. *Clean Coal Technol.* **2010**, *16*, 39–43.